A GENUINELY MULTIDISCIPLINARY JOURNAL
CHEMPLUSCHEM
CENTERING ON CHEMISTRY

Accepted Article

Title: Molecular Wires with Controllable pi-Delocalization Incorporating Redox-triggered Switching Units of pi-Conjugation

Authors: Wataru Nojo, Hitomi Tamaoki, Yusuke Ishigaki, Ryo Katoono, Kenshu Fujiwara, Takanori Fukushima, and Takanori Suzuki

To be cited as: *ChemPlusChem* 10.1002/cplu.201800341

Link to VoR: http://dx.doi.org/10.1002/cplu.201800341

A Journal of ChemPubSoc Europe
WILEY-VCH
www.chempluschem.org

Molecular Wires with Controllable π-Delocalization Incorporating Redox-Triggered π-Conjugated Switching Units

Wataru Nojo,[a] Hitomi Tamaoki,[a] Yusuke Ishigaki,[a] Ryo Katoono,[a] Kenshu Fujiwara,[b] Takanori Fukushima,[c] Takanori Suzuki*[a]

In memory of Shô Itô (1924-2018)

Abstract: A perfluorobiphenyl-2,2'-diyl dication and its corresponding dihydrophenanthrene-type electron donor are interconvertible upon two-electron transfer. Redox-triggered C-C bond-formation/cleavage caused a drastic change in the torsion angle of the biphenyl unit. Thus, π-delocalization ON/OFF switching was observed as a change in the UV spectrum upon electrolysis of the linearly extended analogue with two phenylethynyl groups. A further extended π–system with a molecular length of ca. 3.5 nm, which has two switching units, was synthesized. Spectroelectrograms as well as voltammetric analyses showed that the two units act nearly simultaneously because of the very small inter-unit electrostatic repulsion in the tetracationic state. Thus, the present pair is a promising candidate as a switching unit for the "molecular wires" with controllable π–delocalization, in which a higher ON/OFF ratio of delocalization could be realized by incorporating multiple switching units.

Introduction

Linearly conjugated π–electron systems such as polyynes[1] or polyarylenes[2] are often considered as models for the “molecular wires“.[3] which can conduct electrons along the π–system.[4] On the other hand, they can also "wire" two chromophores at the termini. The electronic communication between the chromophores depends on the nature of the π–components, which consist of repeating units in the main chain structure.[5] When a conjugation-switching unit (“switching unit“) is inserted into the linear π–system, the molecular wire is endowed with the ON/OFF switching properties of π–delocalization to modify the electronic communication along the π–system.[6]

A biaryl-type molecular response system[7] is a promising switching unit since its torsion angle (ϕ) can be controlled by an external stimulus. Thus, the larger degree of π–delocalization is expected when the switching unit adopts a nearly planar structure (“ON-state“), whereas a tightly twisted geometry drives the molecular wire into the “OFF-state“ by disconnecting the effective conjugation (Scheme 1a). Molecular wires with multiple switching units have attracted further attention[8] because a greater ON/OFF ratio regarding π–delocalization is expected due to the simultaneous action of the switching units (Scheme 1b), although only a few examples have been reported so far.

The effectiveness of ON/OFF switching can be evaluated through changes in the delocalization of π–electrons across the switching units. Thus, ON/OFF efficiency can be deduced from the stimulus-induced changes in UV-vis spectra.

Scheme 1.

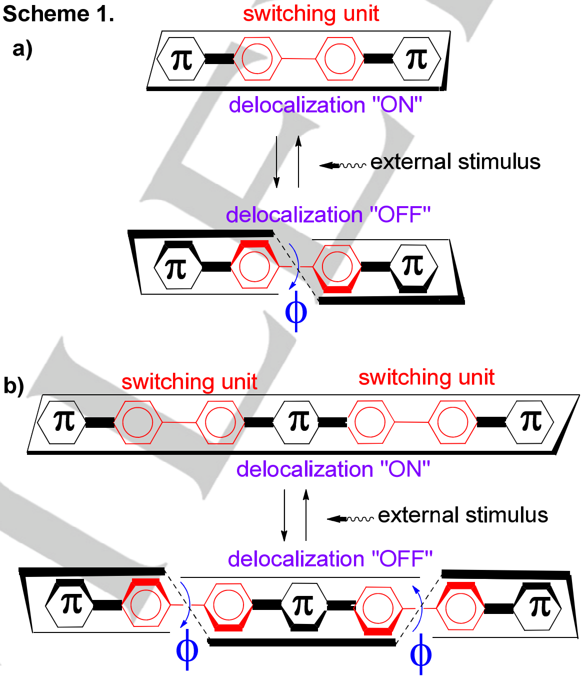

Scheme 1 ON/OFF switching of π-delocalization by geometrical change of the switching unit(s)

Scheme 2.

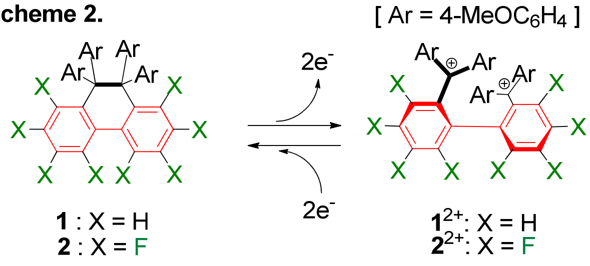

Scheme 2 Dynamic redox systems based on DHP/BP^{2+} skeleton that undergo drastic geometrical change

---

[a] W. Nojo, Dr. H. Tamaoki, Dr. Y. Ishigaki, Dr. R. Katoono, Prof. T. Suzuki
Department of Chemistry, Faculty of Science, Hokkaido University, Sapporo 060-0810 (Japan)
E-mail: tak@sci.hokudai.ac.jp
[b] Prof. K. Fujiwara
Department of Life Science, Graduate School of Engineering, Akita University, Akita, 010-8052 (Japan)
[c] Prof. T. Fukushima
Laboratory for Chemistry and Life Science, Institute of Innovative Research, Tokyo Institute of Technology, Yokohama 226-8503 (Japan)

Supporting information for this article is given via a link at the end of the document: The synthetic details and spectral data of **2**-**6**, **8**, **9** and **11**. UV spectra of **4**, **5**, **6**, **11**, and salts of $\mathbf{2}^{2+}$,$\mathbf{4}^{2+}$ and $\mathbf{5}^{4+}$;geometrical parameters of $\mathbf{2}^{2+}$ in EtOH solvated $\mathbf{2}^{2+}(SbCl_6^-)_2$; DFT calculations of *syn*-**5**, *anti*-**5**, and *syn*-**6**; comparisons of calculated bond lengths in tolane units; cyclic voltammograms of **2**,**4**, and $\mathbf{2}^{2+}$ salt; spectroelectrograms of **5** and **6**, and plausible redox scheme of **5**,**6** to $\mathbf{5}^{4+}$,$\mathbf{6}^{4+}$.

Formula [Ar = 4-MeOC_6H_4]

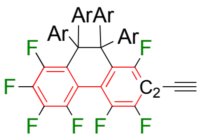

3

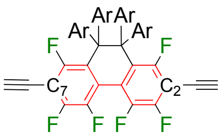

3'

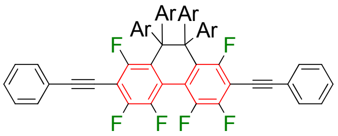

4

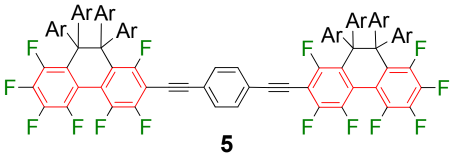

5

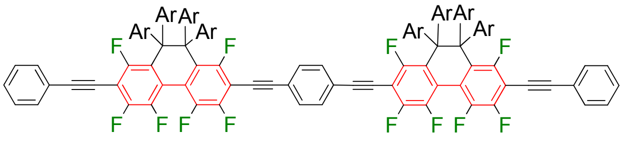

6

Scheme 3.

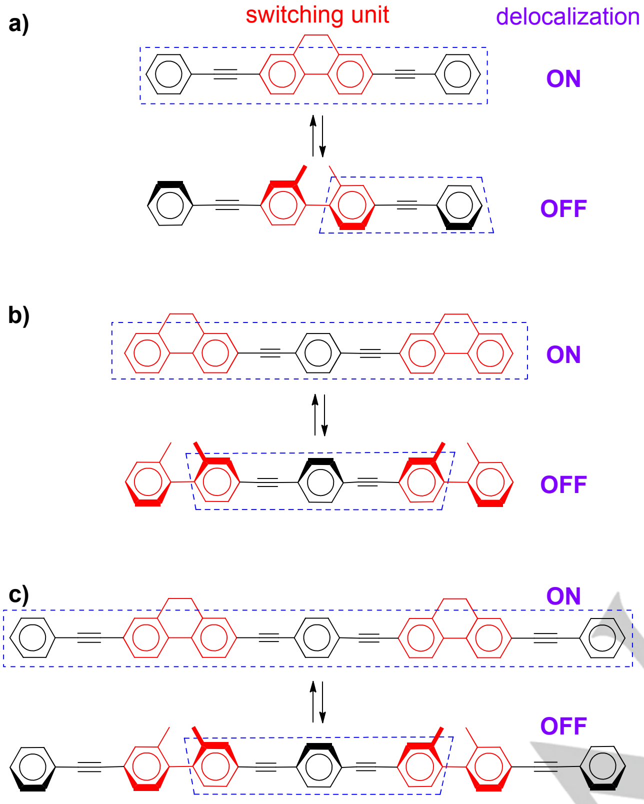

Scheme 3 ON/OFF switching of π-delocalization in the molecular wires with DHP/BP^{2+}-type switching unit(s)

We have shown that the dynamic redox (dyrex) pairs of 9,9,10,10-tetraaryl-9,10-dihydrophenanthrenes (DHP) and biphenyl-2,2'-diyl-type dications (BP^{2+}) such as **1**/**1**$^{2+}$ undergo reversible C-C bond formation/cleavage upon 2e-transfer.[9] Here, we designed a perfluorobiphenyl-based dyrex pair (**2**/**2**$^{2+}$)[10] as a switching unit (Scheme 2), which would undergo S_{NAr} reactions at the F atom(s)[11] with acetylides to give ethynylated derivatives such as **3** or molecular wire **4**. A longer wire with two switching units (**5**) would be synthesized by Pd-catalyzed cross-coupling reactions of **3**. By the further S_{NAr} reaction of **5**, compound **6** would be obtained as the longest wire in this work, with an approximate molecular length of 3.5 nm. Here we report the preparation and redox-dependent spectroscopic properties of **2** - **6**, and discuss the validity of the perfluorobiphenyl-electrophore (**2**/**2**$^{2+}$) in terms of redox-type conjugation switching units.

Results and Discussion

Molecular Design of a Switching Unit (2/2^{2+}) and Molecular Wires 4 - 6.

DHP/BP^{2+}-type dyrex pairs have several advantages as redox-type switching units. First, the biaryl unit in DHP is more or less coplanar (ϕ: ca. 20°)[12] due to the C^9-C^{10} ethano bridge, whereas BP^{2+} adopts a twisted conformation (ϕ: ca. 70°)[9b,13] since the bridging C-C bond is cleaved upon oxidation. Second, in contrast to ordinary organic redox pairs, the facile two-electron transfer occurs nearly at the same potential, which favors high reversibility of the redox processes by reducing the steady-state concentration of the reactive open-shell species.[14] Third, thanks to C-C bond formation/cleavage,[15,16] which causes a drastic change in electronic structures, there is a large potential shift (ca. 1 V) between the oxidation potential (E^{ox}) of DHP and the reduction potential (E^{red}) of BP^{2+}, so that an overpotential is necessary to switch from one state to another.

Effectiveness of conjugation of the biaryl unit can be estimated as $\cos^2\phi$,[17] that determines the degree of π–delocalization over the unit. Thus, the introduction of substituents at the 6,6'-positions of the biphenyl skeleton is desirable to increase the ϕ value for the disconnection of π–conjugation in the BP^{2+} state. Dication **2**$^{2+}$ is an octafluoro derivative of **1**$^{2+}$ (Scheme 2) and would be interconvertible with DHP-type donor **2** upon two-electron transfer. Furthermore, in the dicationic state, the positive charge would not be delocalized into the perfluorobiphenyl skeleton, but rather localized on the bis(4-methoxyphenyl)carbenium moieties. Thus, even when the molecular wire contains multiple switching units, the through-bond electrostatic repulsion could be minimized in the polycationic species. Accordingly, it is highly likely that multiple switching units can work nearly simultaneously in response to an external stimulus (Scheme 1b) to realize a high ON/OFF ratio of π–delocalization.

Molecular wires (**4**, **5**, and **6**) were designed so that the switching unit(s) and other π–system(s) (phenyl, phenylene) are connected with ethynyl bonds in anticipation of their highly coplanar geometries in the ON state. They contain different numbers of benzene rings (4, 5, and 7, respectively) in the main chain. In four-ring system **4**, the redox reaction would cause a drastic change in absorption in the UV region because of the ON/OFF switching of conjugation between the two tolane (1,4-diphenylacetylene) units (Scheme 3a). In five-ring system **5** with two switching units connected by 1,4-diethynylbenzene, the change in UV absorption would be marginal, since only the tetrafluorobenzene termini are twisted (Scheme 3b). However, **5** would provide valuable information on the interaction between the two switching units to confirm their nearly simultaneous action. The longest wire **6** is a unique touchstone for evaluating the proposal in this work by confirming that both switching units actually contribute to ON/OFF switching of the main-chain π-delocalization (Scheme 3c).

Preparation of a Switching Unit (2/2^{2+}) and Molecular Wires 4 - 6.

As shown in Scheme 4, octafluorodiphenoic acid (**8**)[18] derived from 1,2-dibromo-3,4,5,6-tetrafluorobenzene (**7**) was converted into methyl ester **9** in 91% yield. Reaction of **9** with excess 4-$MeOC_6H_4MgBr$ gave tetraarylated diol **10** in 57% yield.

Under acidic dehydrating conditions [HBF_4 - $(CF_3CO)_2O$], diol **10** was transformed into BP^{2+}-type salt, which was directly converted to DHP-type donor **2** as a yellow solid upon treatment with Zn powder in 76% yield over two steps. Through the reaction of **2** with $(4\text{-}BrC_6H_4)_3N^{+\bullet}SbCl_6^-$ (2 equiv.), dication salt $\mathbf{2}^{2+}(SbCl_6^-)_2$ was isolated as a stable entity in 93% yield. The dark red powder of the salt was transformed back to yellow donor **2** upon treatment with Zn powder in 96% yield. This high-yield interconversion indicates that **2** and $\mathbf{2}^{2+}$ can be considered to be a kind of reversible redox pair, similar to non-fluorinated derivatives **1** and $\mathbf{1}^{2+}$ (Scheme 2), although microscopic electrochemical reversibility is not maintained due to concomitant C–C bond-formation/cleavage upon redox reactions (Scheme 5).

We continued our synthesis by taking advantage of the S_{NAr}-reactivity of perfluorobiphenyls that proceeds selectively at the 4,4'-positions,[7a,11a,b] which is desirable for extending the π-conjugation along the long-axis of the biphenyl skeleton. As shown in Scheme 6, the reaction of **2** with ethynyltriisopropylsilane (1.2 equiv.) in the presence of $NaN(SiMe_3)_2$ proceeded at the 2-position of DHP as expected, and detachment of the silyl group gave 2-ethynyl derivative (**3**) in 28% yield over two steps. The relatively low yield can be accounted for if we consider the by-production of 2,7-diethynyl derivat recovery of **2** (ca. 20%).

The reaction of **2** with ethynylbenzene (2.2 equiv.) under similar S_{NAr} conditions gave molecular wire **4** in 40% yield by selective reaction at the 2,7-positions of DHP. Upon oxidation with $(4\text{-}BrC_6H_4)_3N^{+\bullet}SbCl_6^-$ (2 equiv.), dication salt $\mathbf{4}^{2+}(SbCl_6^-)_2$ was isolated as a stable entity in 84% yield, showing that π-extension along the long-axis of the biphenyl unit does not induce fatal instability of the cationic state of the switching unit. Chemical reversibility was confirmed by reducing $\mathbf{4}^{2+}(SbCl_6^-)_2$ with Zn to give **4** in 99% yield.

Next, we sought to synthesize the longer wire **5** under Sonogashira conditions. The reaction of **3** with 1,4-diiodobenzene proceeded smoothly to give **5** (y. 81%), which was isolated as a stable orange solid.[19] Upon the oxidation of **5** with $(4\text{-}BrC_6H_4)_3N^{+\bullet}SbCl_6^-$ (4 equiv.), tetracation salt $\mathbf{5}^{4+}(SbCl_6^-)_4$ was isolated as a stable dark red solid in 77% yield, showing that the incorporation of two switching units does not induce fatal instability of the cationic state of molecular wires. Chemical reversibility was confirmed by reducing $\mathbf{5}^{2+}(SbCl_6^-)_4$ with Zn to give **5** in 93% yield.

By the reaction of **5** with ethynylbenzene (2.2 equiv.) under S_{NAr} conditions, molecular wire **6** was obtained in 43% yield as an orange solid. We noticed that **6** slowly decomposed, especially in solution.

Scheme 4. [Ar = 4-$MeOC_6H_4$]

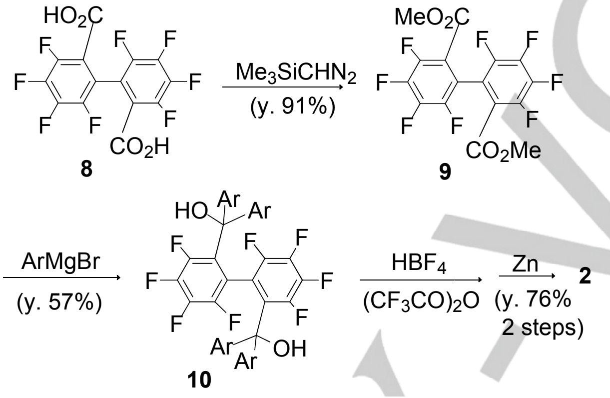

Scheme 4 Synthetic scheme for **2**

Scheme 5. [Ar = 4-$MeOC_6H_4$]

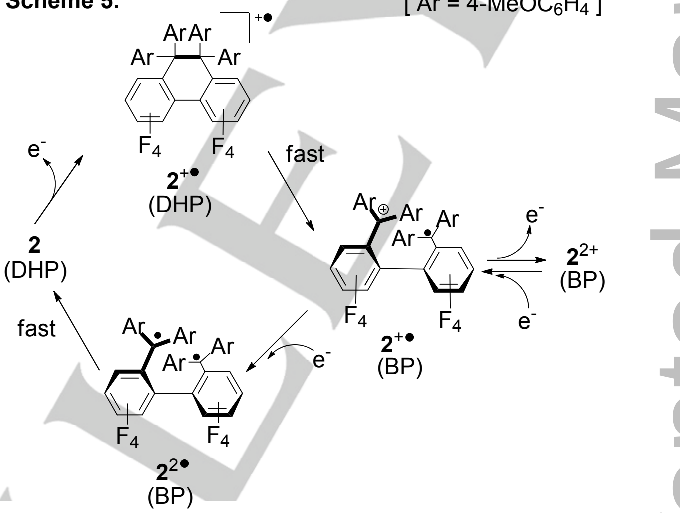

Scheme 5 Mechanism of dyrex interconversion between **2** and $\mathbf{2}^{2+}$

Scheme 6.

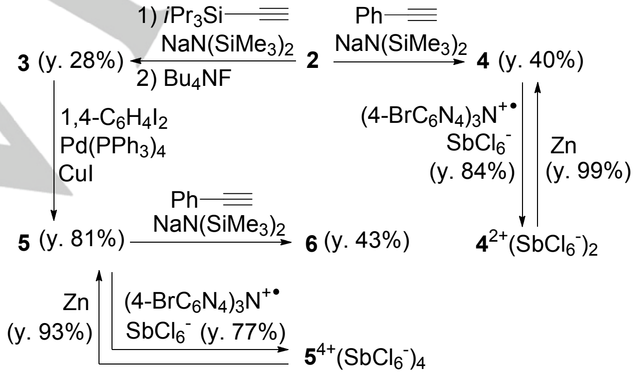

Scheme 6 Synthetic schemes for **3** - **6** as well as interconversion of **4**/$\mathbf{4}^{2+}$ and **5**/$\mathbf{5}^{4+}$.

All of the molecular wires (**4** - **6**) exhibit strong absorptions in the UV region (Table 1, Figure S1). The absorption band of four-ring system **4** (345 nm) is absent in **2** and is assigned to the 4,4'-bis(phenylethynyl)perfluorobiphenyl skeleton.[20] This strong band is red-shifted to 351 nm in the five-ring system **5** and to 357 nm for the seven-ring system **6** due to π–extension along the main chain.[21]

X-ray Structures of the Switching Unit (2/2^{2+})

According to an X-ray analysis, **2** adopts a shallow helical geometry, as in other DHP derivatives (Figure 1a). The torsion angle [<(C4-C4a-C4b-C5)] corresponding to ϕ_{DHP} is 35.1(4)°, which is slightly greater than those of the related molecules[12] due to the F atoms at the bay regions. The C9–C10 bond [1.632(4) Å] is longer than the standard C_{sp3}–C_{sp3} bond (1.54 Å), which is characteristic of sterically congested DHP derivatives.[22]

An X-ray analysis was also conducted for the dication salt of $\mathbf{2}^{2+}(SbCl_6^-)_2$ (Figures 1b and S2). When the C9–C10 bond of **2** is cleaved, the cationic centers are separated by 3.745(9) Å. The two molecular halves are tightly twisted: the torsion angle of the biphenyl skeleton [<(C6-C1-C1'-C6')] is 79.0(1)°, which corresponds to ϕ_{BP}. The central biphenyl bond length is 1.504(7) Å, which is longer than that in neutral **2** [1.480(4) Å] due to disconnection of conjugation. In both triarylmethylium units, each of 4-methoxyphenyl group is connected to the sp^2 cationic plane with a small dihedral angle [17.0(2), 17.5(2), 29.5(2), and 34.4(3)°], whereas the both cationic planes form a larger dihedral angle with the fluoroarene unit [52.6(3) and 56.8(3)°]. The latter values indicate that the positive charges are not delocalized on the perfluorobiphenyl skeleton. This was further confirmed by comparing the bond lengths of C^+ - $C_{ipso(C6H4OMe)}$ [1.406(8), 1.424(8), 1.425(9), and 1.441 (8)] with those of C^+ - $C_{ipso(C6F4)}$ [1.471(9) and 1.498(7) Å], which shows that there is a greater increase in double-bond character in the former bonds.

Thus, X-ray analysis revealed that the dyrex reaction was associated with a large difference between the torsion angles (ϕ_{DHP} and ϕ_{BP}). By considering the $\cos^2\phi$–dependency of the delocalization along the π–system, the expected OFF-state delocalization would be ca. 5% of that in the ON-state (ON/OFF ratio of 18.4). When the two simultaneously-acting switching units are incorporated, the expected OFF-state delocalization would be ca. 0.3% of that in the ON-state (ON/OFF ratio of $18.4^2 = 340$), and thus nearly complete ON/OFF switching would be realized.

DFT Calculations Regarding the Geometrical and Electronic Structures of Molecular Wires 4, 5 and 6

The geometrical and electronic structures of **4** were estimated by DFT calculations (B3LYP/6-31G*). The DHP unit has a molecular geometry (C9-C10 bond length, 1.682 Å; biphenyl bond length, 1.470 Å; torsion angle of biphenyl skeletons: 39.6°) similar to that determined by the X-ray analysis of **2**. The external ethynylbenzene unit is located nearly on the same plane as the trifluoroaryl groups (dihedral angle between the aromatic rings in the tolane units: 3.0 and 0.3°).

Table 1. UV-Vis spectral data measures in MeCN

compound	absorption [λ_{max}/nm (log ε / $M^{-1}cm^{-1}$)]
2	271 (4.15), 230 (4.65).
3	328 (4.62), 265 (4.65), 241 (4.69)
4	345 (4.58), 287 (4.45)
5	351 (4.80)
6	357 (4.90)
$\mathbf{2}^{2+}(SbCl_6^-)_2$	536 (4.79), 392 (4.31), 270 (4.53)
$\mathbf{4}^{2+}(SbCl_6^-)_2$	570sh (4.62), 533 (4.87), 411 (4.45), 318 (4.80), 279 (4.79)
$\mathbf{5}^{4+}(SbCl_6^-)_4$	536 (5.08), 400 (4.68), 337 (4.90), 272 (4.89)

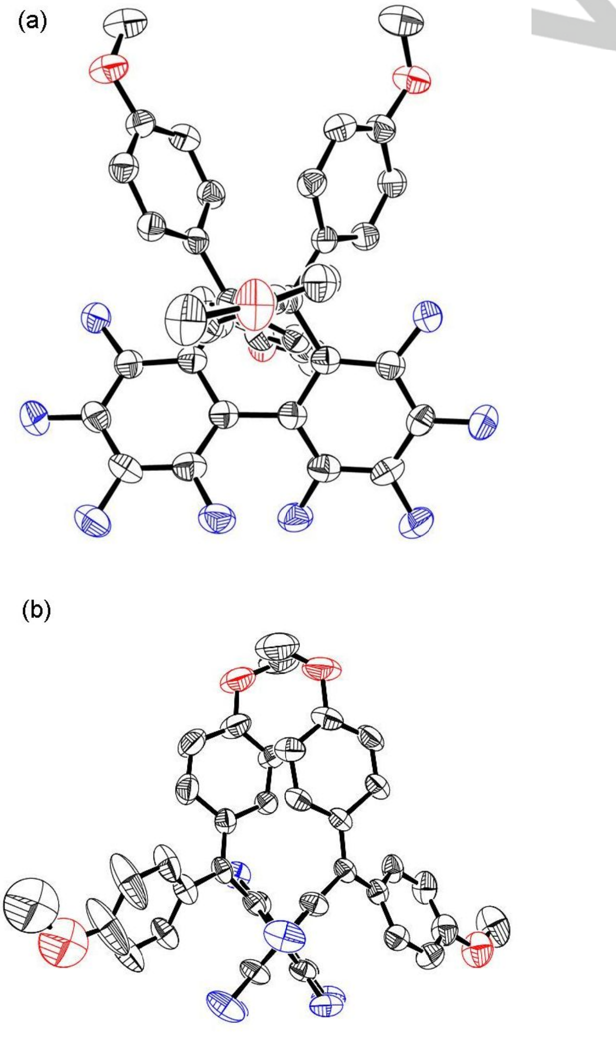

Figure 1. ORTEP drawings of (a) **2** in hexane solvate and (b) $\mathbf{2}^{2+}$ in EtOH solvated $\mathbf{2}^{2+}(SbCl_6^-)_2$ salt.

Scheme 7

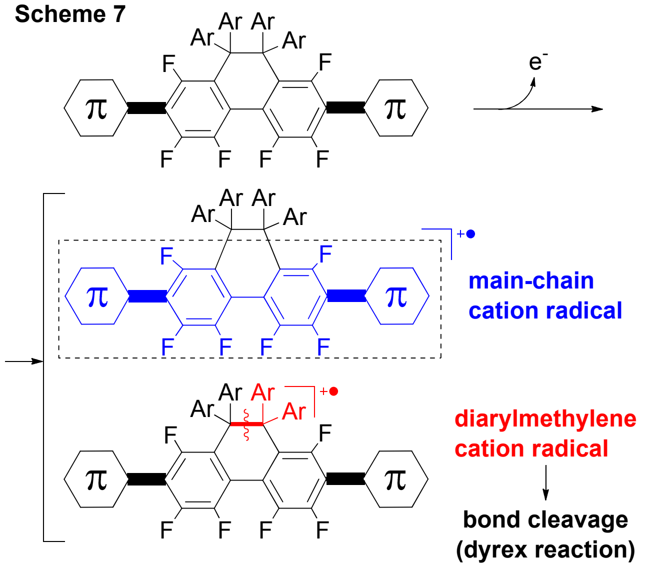

Scheme 7 Two-types of cation radicals in the morecular wires.

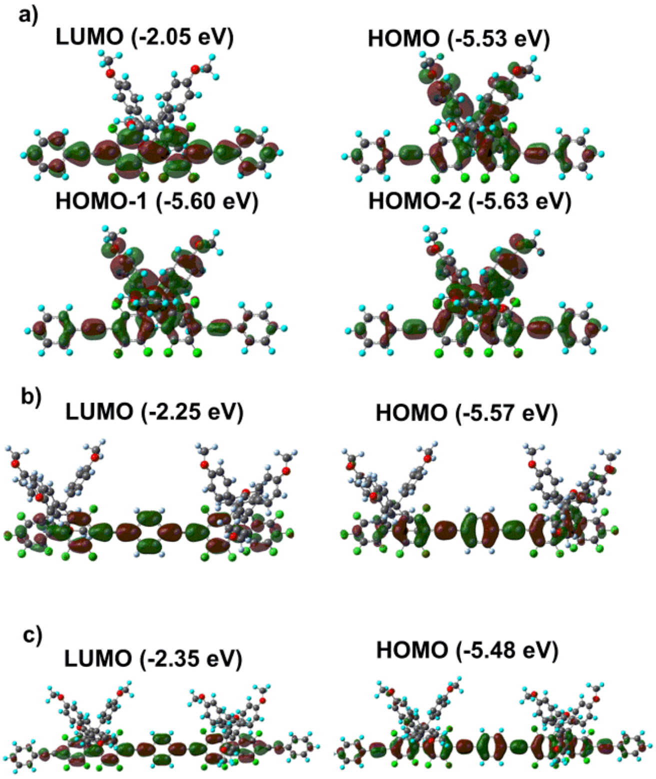

Figure 2. Molecular orbitals and their orbital energies obtained by DFT calculations (B3LYP/6-31G*) on (a) **4**, (b) *syn*-**5** and (c) *syn*-**6**.

The LUMO of **4** mainly shows coefficients on the main-chain ・–system (Figure 2a). HOMO, HOMO-1 and HOMO-2 are nearly degenerated, and have large coefficients on the main-chain as well as on the bis(4-methoxyphenyl)methylene groups of the DHP skeleton. Thus, upon one-electron oxidation of **4**, both the main-chain-type and diarylmethylene-type cation radicals contribute, and the latter is responsible for the dyrex reaction (Scheme 7). Once the C-C bond of the DHP skeleton is cleaved (Scheme 5), the resulting BP-type cation radical is more easily oxidized than **4**, and thus the dyrex reaction may proceed to give $\mathbf{4}^{2+}$.

DFT calculations for **5** with two switching units were carried out for both the *syn*- and *anti*-conformers (Figures S3 and S4), in which the relative orientation of the two switching units is different. The geometrical and electronic structures are very close to each other, and thus only the data for the *syn*-conformer are shown below. Again, each of the DHP units has a slightly helical geometry (torsion angle of biphenyl skeletons: 39.4 and 39.8º). The 1,4-phenylene spacer and the connected trifluoroaryl units exist nearly on the same plane (dihedral angle between the aromatic rings in the tolane units: 1.1 and 0.2º). The HOMO and LUMO mainly show coefficients on this conjugated main-chain ・–system (Figure 2b). HOMO-1, HOMO-2, HOMO-3 and HOMO-4 are nearly degenerated (–5.57 - –5.74 eV), and each has large coefficients on the bis(4-methoxyphenyl)methylene groups of one of the two DHP units (Figure S3). This shows that the main-chain-type cation radical is the major contributor in the longer wire compounds.

This holds true for the longest wire **6** with two additional phenylethynyl units. As designed for the ON state, the main chain is nearly coplanar (torsion angle of the biphenyl skeletons: 39.3 and 39.3°, and the dihedral angle between the aromatic rings in the tolane units: 1.3, 1.7, 3.9, and 4.9º) (Figure S5). Effective π–delocalization of the main chain is confirmed by comparing the bond lengths of the tolane units to those in **4** and **5** (Figure S6). Furthermore, the HOMO and LUMO mainly show coefficients on the main-chain ・–system (Figure 2c), whereas each of the nearly degenerated HOMO-1, HOMO-2, HOMO-3 and HOMO-4 (–5.58 - –5.65 eV) has large coefficients on the bis(4-methoxyphenyl)methylene groups.

These results indicate that longer molecular wires with 1,4-diethynylbenzene and the present switching units would have similar coplanar geometries.[23] The large coefficients of HOMO and LUMO over the main-chain structure are in accord with effective π–delocalization in the ON-state.

Table 2. Redox potentials measured in MeCN[a]

compound	E^{pa}	E^{pc}
2 / $\mathbf{2}^{2+}$	+1.51	+0.30
3 / $\mathbf{3}^{2+}$	+1.51	+0.30
4 / $\mathbf{4}^{2+}$	+1.53	+0.30
5 / $\mathbf{5}^{4+}$	+1.47[b]	+0.30
6 / $\mathbf{6}^{4+}$	ca. +1.5[c]	-[c]

[a] *E* / *V* vs SCE, 0.1 M Et_4NClO_4, Pt electrode, scan rate 500 mV s^{-1}. Ferrocene undergoes one-electron oxidation at +0.38 V under the similar conditions. All of the waves are irreversible, and the anodic peak potential (E^{pa}) in the oxidation wave as well as the cathodic peak potentials (E^{pc}) in the reduction wave are reported. [b] Another peak appeared around ca. 1.6 V (See Figure 3d). [c] Due to less solubility, the peaks are very broad (See Figure 3e).

Redox Properties and Spectroelectrograms of 2 and 4 with One Switching Unit

The electrochemical oxidation of **2** in MeCN occurs at an anodic peak potential (E^{pa}) of +1.51 V vs SCE, which is an irreversible process as in the case of non-fluorinated derivative **1** (+1.50 V).[9b] As expected from the interconversion mechanism shown in Scheme 5, the corresponding cathodic peak is largely shifted to a negative potential region (E^{pc} = +0.30 V) (Figure 3a, Table 2), which corresponds to the 2e-reduction process of $\mathbf{2}^{2+}$ as confirmed by the measurement of the isolated salt of $\mathbf{2}^{2+}$ (Figure S7). This separation of redox peaks is characteristic of dyrex pairs, and favors switching the π–delocalization in molecular wires by demanding overpotentials for switching from one state to another.

Upon electrochemical oxidation in MeCN, the pale yellow solution of **2** turned to a deep purple. The clean conversion of **2** to $\mathbf{2}^{2+}$ as well as a negligible steady-state concentration of open-shell intermediates were confirmed by observing a continuous change with several isosbestic points in the spectroelectrogram (Figure 4a). The strongest absorption appeared in the visible region [λ_{max}/nm (log ε) in MeCN: 536 (4.79) for $\mathbf{2}^{2+}(SbCl_6^-)_2$ (Table 1, Figure S1)], which is characteristic of the bis(4-methoxyphenyl)carbenium skeleton. A similar absorption was observed for non-fluorinated dication $\mathbf{1}^{2+}$ [514 (4.87)]. On the other hand, only a minor change was observed in the UV region upon redox interconversion of the switching unit (**2**/$\mathbf{2}^{2+}$), which suggests that it would be favorable for later studies on molecular wires to scrutinize the changes in UV-region absorption.

Based on the voltammetric analysis, the redox behavior of molecular wire **4** is very close to that of **2** or **3**, with a large separation of redox peaks (Figure 3c), indicating that ・–extension along the long axis of the biphenyl skeleton has only marginal effects on the dyrex behavior of the switching unit. On the other hand, the spectroelectrogram in MeCN (Figure 4b) is dramatically different from that of **2** in the UV-region. The strong band at 345 nm for **4** disappeared upon electrochemical oxidation with a concomitant increase in the blue-shifted band at 318 nm. The latter absorption is similar to that of 2,3,4,5,6-pentafluorotolane (296 nm).[20c] Thus, the redox-induced change in the geometry of the switching unit disconnects the conjugation along the main chain π–system, to give ON-OFF switching of π–delocalization in the four-ring wire **4** (Scheme 3a).

Redox Properties and Spectroelectrograms of 5 and 6 Containing Two Switching Units

When the two switching units in **5** and **6** act nearly simultaneously, a sharp difference in delocalization would be realized for the molecular wires. A major issue is inter-unit interactions,[24] such as electrostatic repulsion, which may interrupt the redox conversion of one unit after another unit is oxidized to the corresponding dication. While both the through-bond and the through-space interactions should be considered, the former interaction is less important because X-ray analysis of $\mathbf{2}^{2+}(SbCl_6^-)_2$ revealed that the delocalization of positive charges into the main-chain component was proven to be minimal.

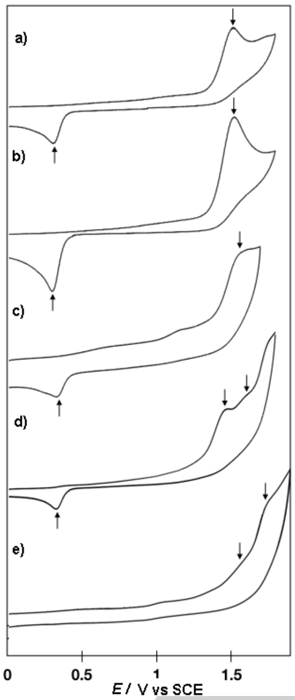

Figure 3. Cyclic voltammograms measured in MeCN: (a) **2**, (b) **3**, (c) **4**, (d) **5**, and (e) **6** (E / V vs SCE, 0.1 M Et_4NClO_4, Pt electrode, scan rate 500 mV s^{-1}.).

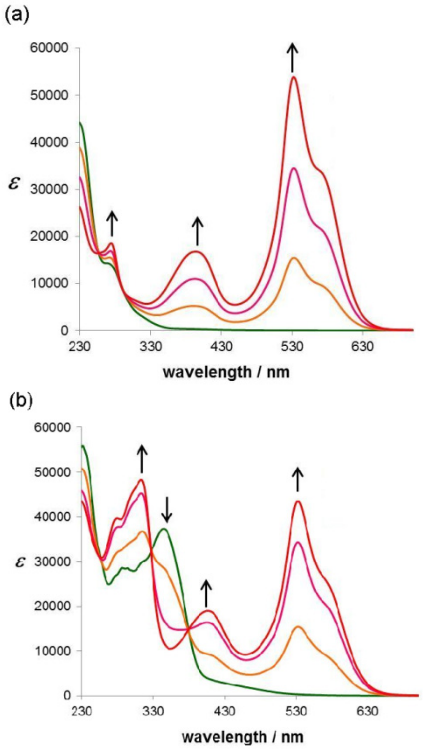

Figure 4. A UV-Vis spectral change upon electrochemical oxidation (60 μA) of (a) **2** (42 μM, every 10 min) and (b) **4** (17 μM, every 5 min) in MeCN containing 0.05 M Et_4NClO_4.

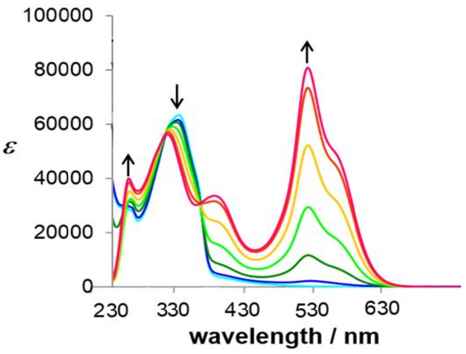

Figure 5. A UV-Vis spectral change upon electrochemical oxidation (60 μA) of **5** (12 μM, every 2 min) in MeCN containing 0.05 M Et_4NClO_4.

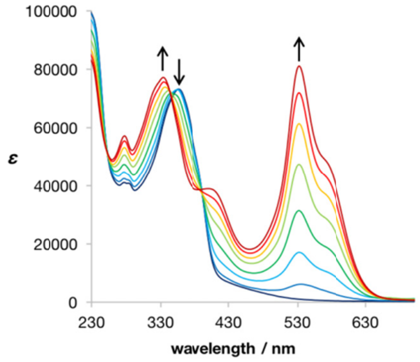

Figure 6. A UV-Vis spectral change upon electrochemical oxidation (20 μA) of **6** (10 μM, every 4 min) in MeCN containing 0.05 M Et_4NClO_4.

To scrutinize the through-space interaction, we first conducted the electrochemical oxidation of **5**. The spectroelectrogram in MeCN exhibits a continuous change (Figure 5) even after the generation of $\mathbf{5}^{4+}$ [λ_{max}/nm (log ε) in MeCN: 536 (5.08) (Table 1)], as suggested by the vis-region absorption,[25] which is much greater than that for the monomeric switching unit in $\mathbf{2}^{2+}$ [536 (4.79)]. A quite similar spectroelectrogram was obtained when electrolysis was conducted in CH_2Cl_2, which does not as effectively stabilize the polycationic state by solvation (Figure S8). Thus, **5** with two switching units could be smoothly and seamlessly oxidized into dication $\mathbf{5}^{2+}$ and then tetracation $\mathbf{5}^{4+}$, suggesting that the through-space electrostatic interaction is marginal, and the molecules of these three redox states (**5**, $\mathbf{5}^{2+}$and $\mathbf{5}^{4+}$) could coexist in the middle of the electrochemical oxidation.

In the voltammogram of **5**, another peak is followed by the first 2e-oxidation peak. Since only poorly resolved shoulders were observed, it is not clear if it could be assigned to the oxidation of $\mathbf{5}^{2+}$ to $\mathbf{5}^{4+}$ (Figure 3d). Even in that case, the potential difference of ca. 0.1 V does not necessarily reflect the electronic structure of cationic species due to the sequential electron-transfer accompanied by multiple bond-cleavage processes (Scheme S1). At any event, the small difference is in line with the negligible electrostatic repulsion suggested for $\mathbf{5}^{4+}$. This is further supported by the fact that E^{pc} of $\mathbf{5}^{4+}$ is nearly the same as that of $\mathbf{2}^{2+}$. The lack of the positive shift of E^{pc} in $\mathbf{5}^{4+}$ indicates that there is no electrostatic repulsion between the two dicationic switching sites.

Due to low solubility, the E^{pa} of **6** appeared less cleanly compared to those of other compounds. According to the DFT calculation (Figure 2c), the main contributor to $\mathbf{6}^{+\bullet}$ is the main-chain-type species (Scheme 7). However, the diarylmethylene-type cation radical should also contribute via the configuration interaction, so that **6** can also undergo facile dyrex reactions as evidenced by the rapid rise in bis(4-methoxyphenylmethylium) absorption upon the electrolysis of **6**. A continuous change was observed in both MeCN (Figure 6) and in CH_2Cl_2 (Figure S8). The spectroelectrograms contain two pseudo isosbestic points, both of which show a gradual change in the wavelength as electrolysis progresses (Figure S9). The observed spectral change can be best accounted for by the sequential oxidation of **6** to $\mathbf{6}^{2+}$ and then to $\mathbf{6}^{4+}$. The solution contains the molecules at these three states, and the proportion of $\mathbf{6}^{4+}$ is increased by the progress of electrochemical oxidation. The strong band of **6** at 361 nm disappeared with a concomitant increase in a new band in the UV-region, the wavelength of which converged to ca. 333 nm, which is close to a strong band of $\mathbf{5}^{4+}(SbCl_6^-)_4$ (337 nm) with the same chromophore in the center of the molecule (Schemes 3b and 3c). Based on these observations, it is highly likely that the new band can be assigned to the 1,4-bis(arylethynyl)benzene-type π–conjugation system,[26] which was generated by changes in the geometries of both switching units upon the conversion of **6** to $\mathbf{6}^{4+}$. We concluded that, in molecular wires with two switching units, both switching units act nearly simultaneously.

Conclusions

In this work, a DHP-BP^{2+}-based dyrex pair was designed as a switching unit to control the π–delocalization along a conjugated main chain for application in future molecular-wire studies. By incorporation of a perfluorobiphenyl skeleton in a dyrex pair, an effective ON/OFF switching ratio was attained with an increased torsion angle especially in the BP^{2+} state. A perfluorobiphenyl skeleton also endows the dyrex pair with S_{NAr} reactivity to connect with another π–system, the selectivity of which is favorable for obtaining linearly-extended molecular wires. According to DFT calculations, the resulting large π–systems have a nearly coplanar geometry for the main chain, on which are located large coefficients of HOMO and LUMO.

Due to redox-triggered C-C bond-formation/cleavage (dyrex behavior), two-electron transfer of the switching units occurs nearly simultaneously to assure the reversibility of redox interconversion, and electrochemical bistability is also favored to keep both the ON and OFF states intact, at least in the absence of an overpotential. Notably, the two switching units in the two-unit system can act nearly simultaneously upon electrochemical oxidation, which could realize complete switching of π–delocalization (ON/OFF ratio = 340).

Experimental Section

Materials and Instruments

^{1}H, ^{19}F and ^{13}C NMR spectra were recorded on BRUKER Ascend TM400 (^{1}H/400 MHz), AMX500 (^{19}F/470 MHz) and JEOL AL300 (^{1}H/300 MHz), α400 (^{13}C/100 MHz), ECA600 (^{1}H/600 MHz, ^{13}C/150 MHz) spectrometers, respectively. IR spectra were obtained on a JEOL JIR-WINSPEC100 FT/IR spectrophotometer. Mass spectra were recorded on a JMS-T100GCV spectrometer in FD and ESI mode. Column chromatography was performed on a silica gel I-6-40 (YMC) with a particle size of 40-63 μm. Melting points were measured on a Yamato MELTING POINT APPARATUS MODEL MP-21 and are uncorrected. UV/Vis spectra were recorded on a HITACHI U-3500 spectrophotometer. Spectroelectrograms were also measured on a U-3500 using YAZAWA CS-12Z for constant-current electrolysis. Cyclic Voltammetry was conducted on a BAS ALS-600A. All commercially available compounds were used without further purification. Solvents were dehydrated prior to use. The synthetic routes for the preparation of **2**-**6**, **8** and **9** are shown in Schemes 2 and 4. Details on their preparation and spectral data are given in the supplementary material.

Redox Potential Measurements

Redox potentials (E^{ox} and E^{red}) were measured by cyclic voltammetry in dry MeCN containing 0.1 mol dm^{-3} Et_4NClO_4 as a supporting electrolyte, respectively. All of the values shown in the text present *E/V* versus SCE measured at a scan rate of 500 mV s^{-1}. A Pt disk electrodes were used as the working and counter electrodes, respectively. The working electrode was polished using a water suspension of Al_2O_3 (0.05 μm) before use.

X-ray Analyses

Crystal data of 2•1/3hexane: MF $C_{44}H_{32.67}F_8O_4$, MW = 777.40, pale yellow prism, 0.10 x 0.10 x 0.10 mm^3, cubic *Ia3bar* (#206), *a* = 27.6408(9) Å, *V* = 21118.0(12) Å^3, ρ (*Z* = 24) = 1.467 g cm^{-1}, *T* = 153 K, μ = 1.212 cm^{-1}. The final *R*1 and *wR*2 values are 0.076 ($I > 2\sigma$) and 0.215 (all data) for 4045 reflections and 252 parameters. Esds for **2** are 0.004-0.005 Å for bond lengths and 0.2-0.3 ° for bond angles, respectively. CCDC 923999.

Crystal data of $2^{2+}(SbCl_6^-)_2$•EtOH: MF $C_{44}H_{34}Cl_{12}F_8O_5Sb_2$, MW = 1463.61, dark red plate, 0.20 x 0.20 x 0.05 mm^3, monoclinic P 21/c (#14), a = 18.0750(2), b = 16.05605(15), c = 20.5277(2)Å, β = 106.9256(12)°, *V* = 5699.37(11) Å^3, ρ (*Z* = 4) = 1.706 g cm^{-1}, *T* = 150 K, μ = 13.290 cm^{-1}. The final *R*1 and *wR*2 values are 0.073 ($I > 2\sigma I$) and 0.230 (all data) for 11487 reflections and 618 parameters. Esds for **2^{2+}** are 0.007-0.015 Å for bond lengths and 0.5-1.3° for bond angles, respectively. CCDC 1849047.

Acknowledgements

We thank Grant-in-Aid for Scientific Research on Innovative Areas: "Middle molecular strategy" (No. 2707) from MEXT and Grant-in-Aid from JSPS (Nos. 15H03790, 16K13968, 18K05069) Japan. This work was also supported by the “Five-star Alliance” in “NJRC Mater. & Dev.” MEXT. .

Keywords: Dyrex System • Electrochromism • Dication • Molecular Device • Molecular Switch

[1] D. C. Milan, M. Krempe, A. K. Ismael, L. D. Movsisyan, M. Franz, I. Grace, R. J. Brooke, W. Schwarzacher, S. J. Higgins, H. L. Anderson, C. L. Lambert, R. R. Tykwinski, R. J. Nichols, *Nanoscale*, **2017**, *9*, 355-361.

[2] (a) C. Sagan, Y. Jiang, F. Caban, J. Snaider, R. Amell, S. Wei, G. M. Florio, *J. Phys. Chem. C* **2017**, *121*, 24945-24953. (b) G. Oektem, K. Sahre, B. Voit, R. Jordan, A. Kiriy, *Polym. Chem.* **2017**, *8*, 2675-2685.

[3] (a) S. Zhen, J. -C. Mao, L. Chen, S. Ding, W. Luo, X. -S. Zhou, A. Qin, Z. Zhao, B. Z. Tnag, *Nano Lett.* **2018**, in press [doi:10.1021/acs.nanolett.8b01082]. (b) N. Algethami, H. Sadeghi, S. Sangtarash, C. J. Lambert, *Nano Lett.* **2018**, in press [doi: 10.1021/acs.nanolett.8b01621]. (c) Y. Yuan, J. -F. Yan, D. -Q. Lin, B. -W. Mao, Y. -F. Yuan, *Chem. Eur. J.* **2018**, *24*, 3545-3555. (d) M. Gantenbein, L. Wang, A. A. Al-Jobory, A. K. Ismael, G. J. Lambert, W. Hong, M. R. Bryce, *Sci. Rep.* **2017**, *7*, 2045-2322. (e) M. Sasaki, T. Koyama, H. Kishida, K. Asaka, Y. Saito, Y. Yoshida, G. Saito, *J. Phys. Chem. Lett.* **2017**, *8*, 1702-1706.

[4] (a) T. Stuyver, T. Zeng, Y. Tsuji, S. Fias, P. Geerlings, F. De Proft, *J. Phys. Chem. C* **2018**, *122*, 2194-3200. (b) Y. Tanaka, M. Kiguchi, M. Akita, *Chem. Eur J* **2017**, *23,* 4741 - 4749. (c) In *Single-Molecule Electronics*, (Ed.: M. Kiguchi), Springer, Singapore, **2016**. (d) M. Di Ventra, In *Electrical Transport in Nanoscale Systems*, Cambridge University Press, Cambridge, **2008.**.

[5] (a) D. Wendinger and R. R. Tykwinski, *Acc. Chem. Res.* **2017**, *50*, 1468-1479. (b) M. Klikar, P. Solanke, J. Tydlitás, and F. Bureš, *Chem. Rec.* **2016**, *16*, 1886-1905. (c) H. Muraoka and S. Ogawa, *Pure Appl. Chem.* **2013**, *85*, 777-784. (d) J. Pina and J. S. S. de Melo, *Phys. Chem. Chem. Phys.* **2009**. *11*, 8706-8713. (e) D. P. Arnold and D. A. James, *J. Org. Chem.* **1997**, *62*, 3460-3469. (f) K. Maruyama and S. Kawabata, *Bull. Chem. Soc. Jpn.* **1989**, *62*, 3498-3507.

[6] (a) J. Andzane, J. Prikulis, d. Dvorsek, D. Mihailovic, D. Erts, *Nanotechnology,* **2010**, *21,* 125706. (b) T. Oike, T. Murata, K. Takimiya, T. Otsubo, Y. Aso, H. Zahng, Y. Araki, O. Ito, *J. Am. Chem. Soc.* **2005**, *127*, 15372-15373. (c) G. K. Ramachandran, T. J. Hopson, A. M. Rawlett, L. A. Nagahara, A. Primak, S. M. Lindsay, *Science*, **2003**, *300*, 1413-1416.

[7] (a) H. Takaoki, R. Katoono, K. Fujiwara, T. Suzuki, **2016**, *Angew. Chem. Int. Ed. 55*, 2582-2586. (b) T. Ohtake, H. Tanaka, T. Matsumoto, M. Kimura, A. Ohta, *J. Org. Chem.* **2014**, *79*, 6590-6602. (c) H. Kurata, S. Kim, T. Fujimoto, K. Matsumoto, T. Kawase, T. Kubo, *Org. Lett.* **2008**, *10*, 3837-3840. (d) J. Nishida, T. Miyagawa, Y. Yamashita, *Org. Lett.* **2004**, *6*, 2623-2526

[8] (a) J. Areephong, J. H. Hurenkamp, M. T. W. Milder, A. Meetsa, J. L. Herek, W. R. Wesley, B. L. Feringa, *Org. Lett.* **2009**, *11*, 721-724. (b) Y. Feng, Y. Yan, S. Wang, W. Zhu, S. Qian, H. Tian, *J. Mat. Chem.* **2006**, *16*, 3685-3692.

[9] (a) T. Suzuki, H. Tamaoki, J. Nishida, H. Higuchi, T. Iwai, Y. Ishigaki, K. Hanada, R. Katoono, H. Kawai, K. Fujiwara, T. Fukushima, in *Organic Redox Systems: Synthesis, Properties and Applications*, *Chapter 2 Redox-mediated reversible σ-bond formation/cleavage*, (Ed.: T. Nishinaga), Wiley, **2015**, pp. 13-38. (b) T. Suzuki, J. Nishida, T. Tsuji, *Angew. Chem. Int. Ed. Engl.* **1997**, *36,* 1329-1331.

[10] (a) A part of this work was reported as a preliminary communication. (b) T. Suzuki, H. Tamaoki, R. Katoono, K. Fujiwara, J. Ichikawa, T. Fukushima, *Chem. Lett.* **2013**, *42*, 703-705.

[11] (a) K. Geramita, Y. Tao, R. a. Segalman, T. D. Tilley, J. Org. Chem. 2010, 75, 1871–1887. (b) K. Geramita, J. McBee, T. D. Tilley, J. Org. Chem. 2009, 74, 820-829. (c) P. L. DeRoy, s. Surprenant, M. Bertrand-Laperie, C. Yoakim, *Org. Lett.* **2007**, *9*, 2714-2743.

[12] (a) T. Suzuki, A. Migita, H. Higuchi, H. Kawai, K. Fujiwara, and T. Tsuji, *Tetrahedron Lett.* **2003**, *44*, 6837-6840. (b) T. Suzuki, J. Nishida, and T. Tsuji, *Chem. Commun.* **1998**, 2193-2194.

[13] T. Suzuki, T. Iwai, E. Ohta, H. Kawai, K. Fujiwara, *Tetrahedron Lett.* **2007**, *48*, 3599-3603.

[14] (a) S. Hünig, M. Kemmer, H. Wenner, I. F. Perepichka, P. Bäuerle, A. Emge, and G. Gesheid, *Chem. Eur. J.* **1999**, *5*, 1969-1973. (b) S. Hünig, M. Kemmer, H. Wenner, F. Barbosa, G. Gesheid, I. F. Perepichka, P. Bäuerle, and A. Emge, *Chem. Eur. J.* **2000**, *6*, 2618-2632. (c) S. Hünig, I. F. Perepichka, M. Kemmer, H. Wenner, P. Bäuerle, and A. Emge, *Tetrahedron* **2000**, *56*, 4203-4211. (d) S. Hünig, C. A. Briehn, P. Bäuerle, and A. Emge, *Chem. Eur. J.* **2001**, *7*, 2745-2757. (e) S. Hünig, S. Aldenkortt, P. Bäuerle, C. A. Briehn, M.

Schäferling, I. F. Perepichka, D. Stalke, and B. Walfort,. *Eur.* J. Org. Chem.**2002**, 1603-1613.

[15] (a) J. K. Mahoney, v. Regnier, E. A. Romero, F. Molton, G. Royal, R. Jazzar, D. Martin, G. Bertrand, *Org. Chem. Front.* **2018** in press (doi: 10.1039/c8qo00447a). (b) H. Yokoi, S. Hiroto, H. Shinokubo, *J. Am. Chem. Soc.* **2018**, *140*, 4649-4655. (c) L. Wojcik, F. Michaud, S. Gauthier, N. Cabon, P. Le Poul, F. Gloaguen, N. Le Poul, *J. Org. Chem.* **2017**, *82*, 12395-12405. (d) J. R. Brandt, L. Pospíšil, L. Bednává. R. Correa de Costa, A. J. White, T. Mori, F. Teplỳ, M. J. Fuchter, *Chem. Commun.* **2017**, *53*, 9059-9062. (e) F. Ba, N. Cabon, P. Le Poul, S. Kahlal, J. -Y. Sailard, N. Le Poul, S. Golhen, D. Caro, F. Robin-Le Guen, *New J. Chem.* **2013**, *37*, 2066-2081. (f) F. Ba, N. Cabon, F. Robin-Le Guen, P. Le Poul, N. Le Poul,Y. Le Mest, S. Golhen, D. Caro, *Organometallics,* **2008**, *27*, 6396-6399.

[16] Reviews: (a) T. Suzuki, H. Tamaoki, J. Nishida, H. Higuchi, T. Iwai, Y. Ishigaki, K. Hanada, R. Katoono, H. Kawai, K. Fujiwara, and T. Fukushima, In *Organic Redox Systems: Synthesis, Properties and Applications, Chapter 2 Redox-mediated reversible* σ*-bond formation/cleavage*, (Ed.: T. Nishinaga), Wiley, 2015, pp. 13-38. (b) T. Suzuki, T. Takeda, E. Ohta, K. Wada, R. Katoono, H. Kawai, and K. Fujiwara, *Chem. Rec.* **2015**, *15*, 280-294. (c) T. Suzuki, E. Ohta, H. Kawai, K. Fujiwara, and T. Fukushima, *Synlett (Account)*, **2007**, 851-869.

[17] (a) In the studies of molecular wires containing biaryl units, the $\cos^2\phi$-dependence of conductance was established (ref. 17b-d), (b) A. Mishchenko, D. Vonlanthen, V. Meded, M. Bürkle, C. Li, I. V. Pobelov, A. Bagrets, J. K. Viljas, F. Pauly, F. Evers, M. Mayor, T. Wandlowski, *Nano Lett.* **2010**, *10*, 156-163. (c) L. Venkataraman, J. E. Klare, C. Nuckolls, M. S. Hybertsen, M. L. Steigerwald, *Nature*, **2006**, *442,* 904-907. (d) S. Woitellier, J. P. Launay, C. Joachim, *Chem. Phys.* **1989**, *131*, 481-488.

[18] R. Filler, A. E. Fiebig, M. Y. Pelister, *J. Org. Chem.* **1980**, *45*, 1290-1295.

[19] Although the shallow helical structure of DHP in **2** causes the stereoisomerism of *P* and *M* in terms of helicity, inversion of the sense of helicity is very fast due to facile ring flipping ($\Delta G^{\neq}$ = 11.0 kcal mol^{-1} for **2**). Thus, **5** can be treated as a single entity without considering their diastereoisomerism among *PP*, *PM,* and *MM.*

[20] (a) Due to fluoro-substitution, this band is red-shifted compared to that for the non-fluorinated 4,4'-bis(phenylethynyl)biphenyl (308 nm in dioxane, ref 20b)]. A similar red shift (from 279 nm to 296 nm in MeCN) was also observed upon 2,3,4,5,6-pentafluoro substitution of tolane (ref 20c). (b) E. Birckner, U.-W. Grummt, A. H. Göller, T. Pautzsch, D. A. M. Egbe, M. Al-Higari, E. Klemm, *J. Phys. Chem. A* **2001**, *105*, 10307-10315. (c) T. A. Zeidan, S. V. Kovalenko, M. Manoharan, R. J. Clark, I. Ghiviriga, I. V. Alabugin, *J. Am. Chem. Soc.* **2005**, *127*, 4270-4285

[21] To confirm the conjugation between the two switching units through 1,4-diethynylbenzene in **5**, its isomer **11** with 1,3-diethynylbenene was prepared for spectral comparisons. By the cross coupling reaction of **3** and 1,3-diiodebenzene, **11** was obtained in 88% yield. Its UV spectrum in MeCN [λ_{max}/nm (log ε) 319 (4.79)] (Figure S1) is quite different from that of **5** with strong band being blue-shifted. Such an observation can be rationalized by the less conjugation of two switching units through 1,3-diethynylbenzene in **11**, which in turn indicates effective conjugation in **5**.

[22] (a) Y. Ishigaki, T. Shimajiri, T. Takeda, R. Katoono, T. Suzuki, *Chem* **2018**, *4*, 795-806. (b) Y. Ishigaki, Y. Hayashi, K. Sugawara, T. Shimajiri, W. Nojo, R. Katoono, T. Suzuki, *Molecules* **2017**, *22*, 1900.

[23] (a) Besides the energy-minimized nearly coplanar conformation shown in Figure 2, partially twisted conformers might coexist for the long chain molecules such as **5** and **6**. Since the twisted conformer has no energy-minimized geometry for the tolane unit (ref. 23b), the non-planar structure for the 1,4-bis(phenylethynyl)benzene unit should be concerned (ref 23c). (b) G. Brizius, K. Billingsley, M. D. Smith, U. H. F. Bunz, *Org. Lett.* **2003**, *5*, 3951-3954. (c) When the DFT calculation of **5** was conducted by using the twisted conformation as an initial structure (dihedral angle between the aromatic rings in the tolane units: 90.0 and 90.0º), the geometrical optimization again converged to the geometry with the nearly planar main-chain structure (*anti*-**5** shown in Figure S4), suggesting that the twisted conformer of 1,4-bis(arylethynyl)benzene has no energy-minimized geometry in the DFT method.

[24] C. Kahlfuss, E. Saint-Aman, C. Bucher, In *Organic Redox Systems: Synthesis, Properties and Applications, Chapter 3 Redox-controlled intramolecular motions triggered by* π*-dimerization and pimerization processes* (Ed.: T. Nishinaga), Wiley, **2015**, pp. 39-88.

[25] If we suppose the same molar extinction coefficient at 536 nm for $\mathbf{5}^{2+}$ to that of $\mathbf{2}^{2+}$, the solution at the later stage of electrolysis contains 70% of $\mathbf{5}^{2+}$ and 30% of $\mathbf{5}^{4+}$, respectively.

[26] Due to fluoro-substitution, this band is red-shifted compared to that for the non-fluorinated 4,4'-bis(phenylethynyl)benzene (320 nm in dioxane, ref 20b)].

Entry for the Table of Contents

FULL PAPER

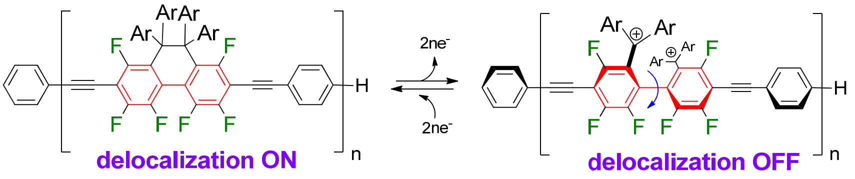

Due to the drastic change in the torsion angle upon 2e-oxidation of tetraaryl-dihydrophenanthrene to biphenyl-2,2'-bis(diarylmethylium), this redox pair can be used as a unique switching unit in linearly extended π–conjugating systems, which were synthesized via S_{NAr}- and cross coupling-reactions. Multiple switching units act nearly simultaneously, and thus promise a higher ON/OFF ratio in molecular wires, the π–delocalization of which can be controlled by an external stimulus.

*Wataru Nojo, Hitomo Tamaoki, Yusuke Ishigaki, Ryo Katoono, Kenshu Fujiwara, Takanori Fukushima and Takanori Suzuki**

Page No. – Page No.

Molecular Wires with Controllable π-Delocalization Incorporating Redox-Triggered π-Conjugated Switching Units